Separation Science and Technology
Publication details, including instructions for authors and subscription information:
http://www.informaworld.com/smpp/title~content=t713708471

Analysis of Separation of Multicomponent Mixtures across Membranes in a Single Permeation Unit

Rishi Bansal[a]; Vipul Jain[a]; Sharad K. Gupta[a]
[a] DEPARTMENT OF CHEMICAL ENGINEERING, INDIAN INSTITUTE OF TECHNOLOGY, NEW DELHI, INDIA

To cite this Article Bansal, Rishi , Jain, Vipul and Gupta, Sharad K.(1995) 'Analysis of Separation of Multicomponent Mixtures across Membranes in a Single Permeation Unit', Separation Science and Technology, 30: 14, 2891 — 2916
To link to this Article: DOI: 10.1080/01496399508013721
URL: http://dx.doi.org/10.1080/01496399508013721

SEPARATION SCIENCE AND TECHNOLOGY, **30**(14), pp. 2891–2916, 1995

Analysis of Separation of Multicomponent Mixtures across Membranes in a Single Permeation Unit

---

RISHI BANSAL, VIPUL JAIN, and SHARAD K. GUPTA*
DEPARTMENT OF CHEMICAL ENGINEERING
INDIAN INSTITUTE OF TECHNOLOGY, DELHI
HAUZ KHAS, NEW DELHI 110016, INDIA

ABSTRACT

A method for the numerical simulation of separation of multicomponent gaseous mixtures across membranes is developed. It is shown that the governing differential equations for the plug flow geometries (crossflow, cocurrent flow, and countercurrent flow) are identical in form and can be reduced to a single general equation. The only difference lies in the manner the mole fraction of each component on the permeate side depends on its feed side composition at each point along the membrane. There are three important dimensionless factors, the pressure ratio, the permeabilities relative to that of the most permeable component, and either the stage cut or the dimensionless area, which describe the operation of the permeation unit. The method is equally amenable to cases for which the area is known and for which the stage cut is known. The separation of a binary mixture of N_2 and O_2 in all four flow geometries and of a mixture of H_2, CH_4, CO, and CO_2 in full mixing are simulated by the methods of the present study. The results obtained are in good agreement with the values in the literature. The method is repeated for the simulation of separation of a mixture containing H_2, N_2, O_2, and CH_4 for all four flow geometries.

INTRODUCTION

In the past few years, considerable progress has been made in various aspects of membrane technology, particularly in the field of gas separation. This is the result of better understanding of the interrelationships

---

* To whom correspondence should be addressed.

between the structure and properties of the membranes. Advances have also been made in the design and fabrication of gas permeation units.

Current applications of membrane separation include removal of SO_2 from flue gases, H_2 and CO separation from synthesis gases, separation of product gas from reaction gases, and separation of hydrogen from a gas refinery stream. In most of these applications the multicomponent nature of the feed is evident. Most of the previous papers on gas separation (1–8) considered binary gas mixtures. Moreover, in these studies the stage cut was assumed known beforehand and then the permeate and retentate concentrations, as well as the membrane area, were calculated. In many applications such as the design of multistage permeation units, the area of the membrane in a single permeation stage is often known and the resulting stage cut and concentrations have to be computed.

There are some reports about multicomponent gas mixtures (3, 5), but these either deal with a limited number of components, with perfect mixing, or with special cases [such as a nonpermeable component along with two permeable components (9)], which have been discussed for various geometries. In Reference 3 the analysis of multicomponent gas separation for the full mixing case was discussed for any number of components with a known stage cut.

The present study is a theoretical analysis for multicomponent gas separation with four different flow geometries:

1. Cocurrent
2. Countercurrent
3. Crossflow
4. Full mixing

A different solution for full mixing flow geometry is presented. For each flow geometry, solutions are presented for the area with known stage cut and vice versa. Numerical simulation is carried out to study the effect of the various operating conditions, flow geometries, permeabilities, and feed concentrations.

THEORY

The single permeation stage as shown in Fig. 1(a) is divided into two parts by a membrane of constant permeabilities K_is, area A, width W, and membrane thickness δ. The feed Q^f enters the unit and is finally divided into two streams: Q^o leaving on the retentate side and Q^p on the permeate side. The mole fractions in these streams are x_i^f, x_i^o, and y_i^p,

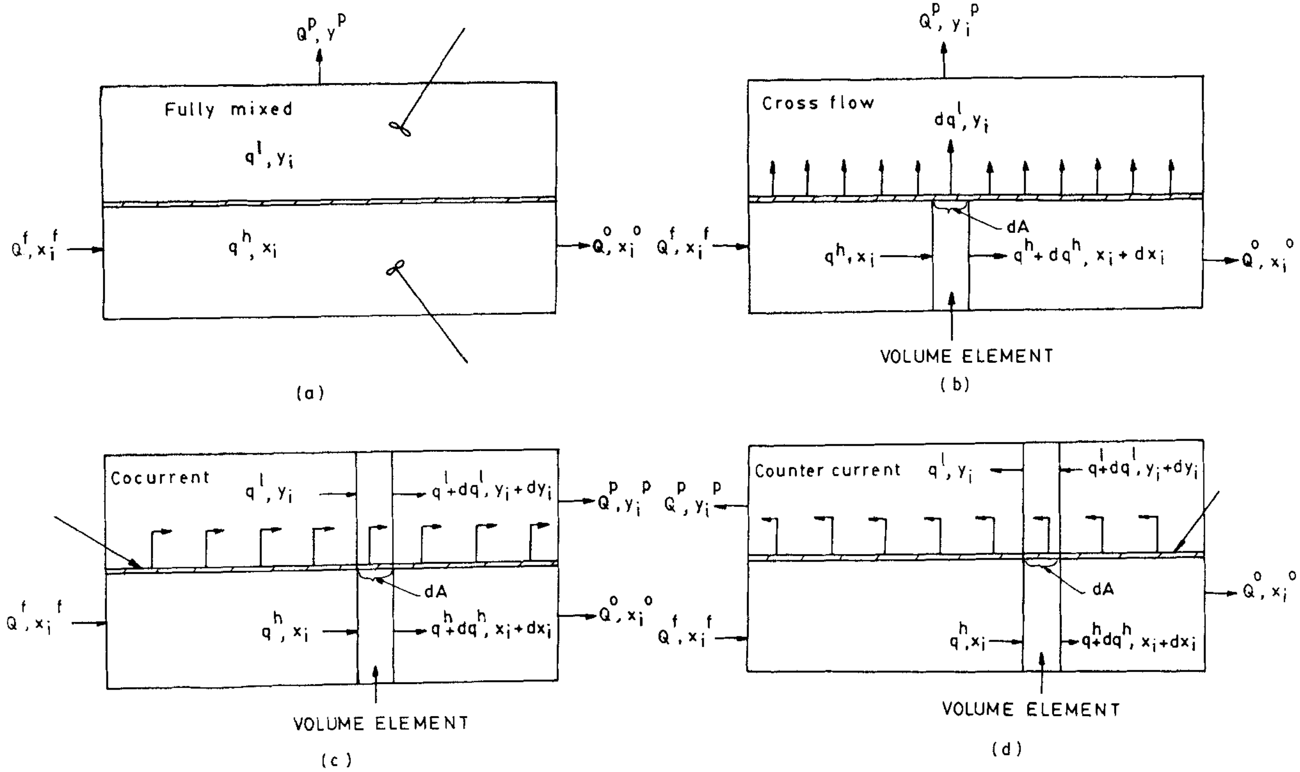

FIG. 1 Flow geometries.

respectively. Hence

$$\sum_{i=1}^{n} x_i^{\mathrm{f}} = 1 \tag{1}$$

$$\sum_{i=1}^{n} x_i^{\mathrm{o}} = 1 \tag{2}$$

$$\sum_{i=1}^{n} y_i^{\mathrm{p}} = 1 \tag{3}$$

Without the loss of generality, it is assumed that the permeabilities are arranged in descending order, i.e.,

$$K_1 > K_2 > \cdots > K_i > K_{i+1} > \cdots > K_n$$

The following assumptions have been made while carrying out the analysis:

1. The permeability of each component is the same as that of the pure species and is independent of pressure.
2. Steady state is assumed.
3. The membrane is of uniform thickness.
4. The total pressure on each side of the membrane is essentially constant.
5. In the direction perpendicular to the membrane, there are no concentration gradients.
6. In all cases other than full mixing, plug flow is assumed.

The overall mass balance can be written as

$$Q^{\mathrm{f}} = Q^{\mathrm{p}} + Q^{\mathrm{o}} \tag{4}$$

Similarly, the component balances can be written as

$$Q^{\mathrm{f}}x_i^{\mathrm{f}} = Q^{\mathrm{p}}y_i^{\mathrm{p}} + Q^{\mathrm{o}}x_i^{\mathrm{o}} \tag{5}$$

The stage cut is defined as

$$\phi = \frac{Q^{\mathrm{p}}}{Q^{\mathrm{f}}} = \frac{Q^{\mathrm{f}} - Q^{\mathrm{o}}}{Q^{\mathrm{f}}} \tag{6}$$

Equations (4), (5), and (6) are applicable to all four flow geometries. We now consider each flow geometry separately.

FULL MIXING

This case is shown in Fig. 1(a). The streams on both sides of the membrane are fully mixed, and no concentration gradients are present within each section. A method of solution for this case has been given by Shindo (3). However, this analysis is applicable only when the stage cut is known beforehand. The alternate method presented here is able to handle cases of known stage cut (but unknown area) as well as that of unknown stage cut (but known area).

On the basis of a full mixing assumption, the following equations can be obtained for each component present in the mixture.

$$Q^{\mathrm{p}} y_i^{\mathrm{p}} = \frac{K_i A}{\delta}\,(P_{\mathrm{h}} x_i^{\mathrm{o}} - P_{\mathrm{l}} y_i^{\mathrm{p}}) \tag{7}$$

Using Eqs. (3) and (7), we obtain

$$Q^{\mathrm{p}} = \sum_{i=1}^{n} \frac{K_i A}{\delta}\,(P_{\mathrm{h}} x_i^{\mathrm{o}} - P_{\mathrm{l}} y_i^{\mathrm{p}}) \tag{8}$$

By combining Eqs. (4), (5), and (6), we obtain the following equation for the stage cut:

$$\phi = \frac{x_i^{\mathrm{o}} - x_i^{\mathrm{f}}}{x_i^{\mathrm{o}} - y_i^{\mathrm{p}}} \tag{9}$$

Now, using Eqs. (6), (7), (9), and rearranging, we obtain

$$x_i^{\mathrm{o}} = \frac{x_i^{\mathrm{f}}\left[\phi Q^{\mathrm{p}} + \left(\dfrac{P_{\mathrm{l}} K_i A}{\delta}\right)\right]}{\left[\left(\dfrac{K_i A}{\delta}\right)(\phi P_{\mathrm{h}} + P_{\mathrm{l}}(1 - \phi)) + (\phi - \phi^2) Q^{\mathrm{p}}\right]} \tag{10}$$

Thus x_i^{o} has been obtained in terms of inlet feed concentrations (x_i^{f}), operating conditions, area, and stage cut. Of these parameters, only either area or stage cut is unknown. Since

$$\sum_{i=1}^{n} x_i^{\mathrm{o}} = 1 \tag{2}$$

we may write

$$F(\phi, A) = \sum_{i=1}^{n} x_i^{\mathrm{o}} - 1 = 0 \tag{11}$$

where x_i^0 is given by Eq. (10) subject to the condition that it lies between 0 and 1.

The value of either ϕ or A is known, so in Eq. (11) there is only a single unknown, either ϕ or A, which can be determined numerically. The function $F(\phi, A)$ becomes an implicit function of the single variable. Equation (11) will have a root in the interval between the limiting values of the unknown variable. These limiting values can be calculated as shown in Appendix 1. The interval is divided into a number of equally spaced subintervals and searched for zero crossings of the function $F(\phi, A)$; a pair of bracketing values is found (11). In this pair the function changes sign. But in doing so a problem may be encountered: During the evaluation of $F(\phi, A)$, the values of x_i^0s calculated for certain values of the unknown variable by using Eq. (10) may either exceed unity or be less than 0. These values of the unknown variable must be carefully discarded during simulation.

CROSSFLOW

This case is shown in Fig. 1(b). In this flow geometry the stream on the permeate side flows perpendicular to the membrane and away from it. On the retentate side the gas stream flows parallel to the membrane and away from the feed point. No mixing takes place on either side of the membrane. Previous work in this case deals primarily with binary mixtures.

By considering the differential area element dA, the following mass balance equations can be easily written:

$$dq^{\mathrm{h}} = -dq^{\mathrm{l}} \tag{12}$$

$$d(q^{\mathrm{h}}x_i) = -y_i dq^{\mathrm{l}} \tag{13}$$

and

$$y_i dq^{\mathrm{l}} = \left[\frac{dA}{\delta}\right] K_i(P_{\mathrm{h}}x_i - P_{\mathrm{l}}y_i) \tag{14}$$

Since $\Sigma x_i = 1$ and $\Sigma y_i = 1$, we may use Eqs. (12), (13), and (14) to obtain

$$\frac{dq^{\mathrm{l}}}{dA} = -\frac{dq^{\mathrm{h}}}{dA} = \sum_{i=1}^{n} \left\{\frac{K_i}{\delta}(P_{\mathrm{h}}x_i - P_{\mathrm{l}}y_i)\right\} \tag{15}$$

Also

$$\frac{d(q^{\mathrm{h}}x_i)}{dA} = q^{\mathrm{h}}\frac{dx_i}{dA} + x_i\frac{dq^{\mathrm{h}}}{dA} \tag{16}$$

Now, using Eqs. (13), (14), and (15), Eq. (16) simplifies to

$$\frac{dx_i}{dA} = \frac{\left[x_i\sum_{j=1}^{n}\frac{K_i}{\delta}(P_{\mathrm{h}}x_{\mathrm{j}} - P_{\mathrm{l}}y_{\mathrm{j}})\right] - \frac{K_i}{\delta}(P_{\mathrm{h}}x_i - P_{\mathrm{l}}y_i)}{q^{\mathrm{h}}} \tag{17}$$

When there is no gas into the differential volume element on the permeate side parallel to the membrane, then the permeate mole fractions y_is are functions only of feed side mole fractions, which can be evaluated as shown in Appendix 2. Thus

$$y_i = f(x_1, x_2, x_3, \ldots, x_n, i) \equiv f(\{x_i\}, i) \tag{18}$$

Using Eq. (18), Eqs. (15) and (17) can be rewritten as

$$\frac{dq^{\mathrm{h}}}{dA} = -\sum_{i=1}^{n}\left\{\frac{K_i}{\delta}(P_{\mathrm{h}}x_i - P_{\mathrm{l}}f(\{x_i\}, i)\right\} \tag{19}$$

and

$$\frac{dx_i}{dA} = \frac{\left[x_i\sum_{j=1}^{n}\frac{K_i}{\delta}(P_{\mathrm{h}}x_j - P_{\mathrm{l}}f(\{x_i\}, i))\right] - \frac{K_i}{\delta}(P_{\mathrm{h}}x_iP_{\mathrm{l}}f(\{x_i\}, i))}{q^{\mathrm{h}}} \tag{20}$$

Equation (20) holds for each component. Thus with Eq. (19) we have $(n + 1)$ coupled differential equations in $(n + 1)$ variables, and the initial conditions are

$$x_i|_{A=0} = x_i^{\mathrm{f}} \quad \text{and} \quad q^{\mathrm{h}}|_{A=0} = Q^{\mathrm{f}}$$

i.e., the mole fractions and flow rate at the feed point on the retentate side are the same as those for the feed itself.

This is an initial value problem which can be solved by any numerical scheme such as the Runge Kutta method.

When the area is known, it is divided into an adequate number of steps and integration is carried out to obtain the value of Q^{o}, and x_i^{o}s, y_i^{p}s, and ϕ can be obtained by using Eqs. (4), (5), and (6), respectively.

When ϕ is known, a suitable step area is chosen and the equations are integrated until q^{h} is equal to Q^{o}. The value of area obtained is the required membrane area. From the x_i^os thus obtained, y_i^ps can be calculated using Eq. (5).

COCURRENT

This case is shown schematically in Fig. 1(c). The gas streams on both sides of the membrane flow parallel to it and in the same direction. This case has been discussed in detail for binary mixtures (1, 6, 7). Pan and Habgood (9) extended it to include a nonpermeable component along with two permeable components. The present study discusses the case for any number of components.

Considering the differential area element dA, the following equations can be obtained:

$$Q^{\mathrm{f}} = q^{\mathrm{h}} + q^{\mathrm{l}} \tag{21}$$

$$Q^{\mathrm{f}}x_i^{\mathrm{f}} = q^{\mathrm{h}}x_i + q^{\mathrm{l}}y_i \tag{22}$$

$$dq^{\mathrm{h}} = -dq^{\mathrm{l}} \tag{23}$$

$$d(q^{\mathrm{h}}x_i) = -d(q^{\mathrm{l}}y_i) \tag{24}$$

$$d(q^{\mathrm{l}}y_i) = \left[\frac{dA}{\delta}\right] K_i(P_{\mathrm{h}}X_i - P_{\mathrm{l}}y_i) \tag{25}$$

$$\frac{d(q^{\mathrm{h}}x_i)}{dA} = -\frac{K_i}{\delta}(P_{\mathrm{h}}x_i - P_{\mathrm{l}}y_i) \tag{26}$$

Summing over the components from Eq. (26), the following equation can be easily obtained.

$$\frac{dq^{\mathrm{h}}}{dA} = -\sum_{i=1}^{n}\left[\frac{K_i}{\delta}(P_{\mathrm{h}}x_i - P_{\mathrm{l}}y_i)\right] \tag{27}$$

Using Eqs. (16), (25), and (26), the following equation is obtained for x_is.

$$\frac{dx_i}{dA} = \frac{\left[x_i\sum_{j=1}^{n}\frac{K_j}{\delta}(P_{\mathrm{h}}x_j - P_{\mathrm{l}}y_j)\right] - \frac{K_i}{\delta}(P_{\mathrm{h}}x_i - P_{\mathrm{l}}y_i)}{q^{\mathrm{h}}} \tag{28}$$

Now, from Eqs. (21) and (22) we have

$$y_i = \frac{Q^{\mathrm{f}}x_i^{\mathrm{f}} - q^{\mathrm{h}}x_i}{Q^{\mathrm{f}} - q^{\mathrm{h}}}, \qquad Q^{\mathrm{f}} \neq q^{\mathrm{h}}$$

When $Q^f = q^h$, then $q^l = 0$, and the condition for application of Eq. (18) is satisfied and may be used for determining y_is. Thus

$$y_i = \begin{cases} \dfrac{Q^f x_i^f - q^h x_i}{Q^f - q^h}, & Q^f \neq q^h \\ f(x_1, x_2, x_3, \ldots, x_n, i) \equiv f(\{x_i\}, i), & Q^f = q^h \end{cases} \tag{29}$$

Equations (27) and (28) along with Relations (29) form a set of $(n + 1)$ coupled differential equations. The initial conditions for the differential equations are

$$x_i|_{A=0} = x_i^f \quad \text{and} \quad q^h|_{A=0} = Q^f$$

These equations can be integrated from $A = 0$ to $A =$ area for the case of known area. For known ϕ the integration is carried out until the desired flow rates are obtained. Once x_i^os are known, y_i^ps can be found from Eq. (5).

COUNTERCURRENT

This case is shown schematically in Fig. 1(d). Except for the fact that gas streams flow in opposite directions, the case is similar to the cocurrent case. The literature for this case parallels that for the cocurrent case (1, 6, 7). The mass balance equations for this flow geometry are given below.

$$q^h - q^l = Q^f - Q^p = Q^o \tag{30}$$

$$q^h x_i - q^l y_i = Q^f x_i^f - Q^p y_i^p = Q^o x_i^o \tag{31}$$

$$dq^h = dq^l \tag{32}$$

$$d(q^h x_i) = d(q^l y_i) \tag{33}$$

$$\frac{d(q^l x_i)}{dA} = -\frac{K_i}{\delta}(P_h x_i - P_l y_i) \tag{34}$$

From Eqs. (33) and (34) we have

$$\frac{dq^h}{dA} = -\sum_{i=1}^{n}\left[\frac{K_i}{\delta}(P_h x_i - P_l y_i)\right] \tag{35}$$

and following the method for the cocurrent case, we have

$$\frac{dx_i}{dA} = \frac{\left[x_i \sum_{j=1}^{n} \frac{K_i}{\delta}(P_h x_j - P_l y_j)\right] - \frac{K_i}{\delta}(P_h x_i - P_l y_i)}{q^h} \tag{36}$$

where the y_is are given by

$$y_i = \begin{cases} \dfrac{q^h x_i + Q^p y_i^p - Q^f x_i^f}{q^h + Q^p - Q^f}, & q^h + Q^p \neq Q^f \\ f(x_1, x_2, x_3 \ldots, x_n, i) \equiv f(\{x_i\}, i), & q^h + Q^p = Q^f \end{cases} \tag{37}$$

Here Q^p and y_i^ps are unknown and can be obtained only after the results of integration are known. The $(n + 1)$ differential equations can be solved by using the shooting method to adjust for the values of unknowns at the feed point.

However, it is convenient to shift the origin of the problem to the exit of retentate. Equation (37) can be reframed in the form

$$y_i = \begin{cases} \dfrac{q^h x_i - Q^o x_i^o}{q^h - Q^o}, & q^h \neq Q^o \\ f(\{x_i\}, i), & q^h = Q^o \end{cases} \tag{38}$$

Equations (35) and (36) together with Relations (38) constitute a boundary value problem. This is solved from right to left with the value of the area arbitrarily assigned zero at the beginning, and after integration the sign of the area obtained is reversed.

The initial guesses are now made at the exit point and the problem solved as an initial value problem. The values resulting at the feed point will not in general match those given in the problem. The shooting method (11) is used to adjust each initial guess to its correct value. In this method the value of each guess is adjusted by observing the effect it produces on the final match.

For the case of unknown ϕ, initial guesses for the values of x_i^os have to be made and refined, while for the case of known area, guesses for Q^o have also to be made. In the absence of other information, the values obtained for the cocurrent case form a reasonable guess.

Values of y_i^ps are calculated by the method identical to that used in the cocurrent case.

DIMENSIONLESS ANALYSIS

In spite of the considerable differences in the flow geometries, there is an underlying mathematical similarity among the cases of crossflow, cocurrent flow, and countercurrent flow. It can be clearly seen that Eqs. (19) and (20), (27) and (28), and (35) and (36), which are the governing differential equations for the crossflow, cocurrent flow, and countercurrent flow cases, respectively, are identical in form, i.e.,

$$\frac{dq^{\mathrm{h}}}{dA} = -\sum_{i=1}^{n}\left[\frac{K_i}{\delta}(P_{\mathrm{h}}x_i - P_{\mathrm{l}}y_i)\right] \qquad (19, 27, 35)$$

$$\frac{dx_i}{dA} = \frac{\left[x_i\sum_{j=1}^{n}\frac{K_j}{\delta}(P_{\mathrm{h}}x_j - P_{\mathrm{l}}y_j)\right] - \frac{K_i}{\delta}(P_{\mathrm{h}}x_i - P_{\mathrm{l}}y_i)}{q^{\mathrm{h}}} \qquad (20, 28, 36)$$

Introducing the dimensionless quantities

$$\mathrm{Pr} = P_{\mathrm{l}}/P_{\mathrm{h}} \qquad (39)$$

$$\gamma_i = K_i/K_1 \qquad (40)$$

$$\bar{q}^{\mathrm{h}} = q^{\mathrm{h}}/Q^{\mathrm{f}} \qquad (41)$$

$$\bar{A} = \frac{AK_1P_{\mathrm{h}}}{\delta Q^{\mathrm{f}}} \qquad (42)$$

where γ_i is the ideal separation factor of the ith component with respect to the most permeable component, $\bar{q}^{\mathrm{h}}$ is the dimensionless flow rate, and $\bar{A}$ is the dimensionless area. Governing equations in terms of these dimensionless variables become

$$\frac{d\bar{q}^{\mathrm{h}}}{d\bar{A}} = -\sum_{i=1}^{n}[\gamma_i(x_i - \mathrm{Pr}y_i)] \qquad (43)$$

$$\frac{dx_i}{d\bar{A}} = \frac{x_i\left[\sum_{j=1}^{n}\gamma_j(x_j - \mathrm{Pr}y_j)\right] - \gamma_i(x_i - \mathrm{Pr}y_i)}{\bar{q}^{\mathrm{h}}} \qquad (44)$$

The boundary conditions for these equations are

$$x_i|_{\bar{A}=0} = x_i^{\mathrm{f}} \qquad (45)$$

$$\bar{q}^{\mathrm{h}}|_{\bar{A}=0} = 1 \qquad (46)$$

The solutions for these three cases differ only inasmuch as the functional relationship of y_i with x_i is different. In terms of dimensionless quantities, these relationship can be expressed as:

1. Crossflow:

$$y_i = f(x_1, x_2, \ldots, x_n, \mathrm{Pr}) \equiv f(\{x_i\}, \mathrm{Pr}) \qquad \text{(see Appendix 2)} \quad (47)$$

2. Cocurrent flow:

$$y_i = \begin{cases} \dfrac{x_i^{\mathrm{f}} - \bar{q}^{\mathrm{h}}x_i}{1 - \bar{q}^{\mathrm{h}}}, & \bar{q}^{\mathrm{h}} \neq 1 \\ f(\{x_i\}, \mathrm{Pr}), & \bar{q}^{\mathrm{h}} = 1 \end{cases} \qquad (48)$$

3. Countercurrent flow:

$$y_i = \begin{cases} \dfrac{\bar{q}^{\mathrm{h}} x_i + \phi y_i^{\mathrm{p}} - x_i^{\mathrm{f}}}{\bar{q}^{\mathrm{h}} + \phi - 1}, & \bar{q}^{\mathrm{h}} \neq 1 - \phi \\ f(\{x_i\}, \mathrm{Pr}), & \bar{q}^{\mathrm{h}} = 1 - \phi \end{cases} \tag{49}$$

When $\mathrm{Pr} = 0$, then the governing equations become independent of y_i and hence reduce to the same mathematical form. Therefore the permeate side flow pattern ceases to have any effect on the solution.

For the full mixing case the basic Eqs. (10) and (11) can be reduced to

$$x_i^{\mathrm{o}} = \frac{x_i^{\mathrm{f}}[\phi^2 + \bar{A}\mathrm{Pr}\gamma_i]}{[\gamma\bar{A}(\phi + \mathrm{Pr}(1 - \phi)) + (1 - \phi)\phi^2]} \tag{50}$$

$$F(\phi, \bar{A}) = \sum_{i=1}^{n} x_i^{\mathrm{o}} - 1 = 0 \tag{51}$$

It can be seen from Eqs. (43) to (51) that the achievable degree of separation for a multicomponent gas mixture in a single permeation stage for a given stage cut depends only on the ideal separation factors γ_is, the pressure ratio Pr, and the choice of the flow pattern. This result was reported for the binary case by Walawender and Stern (7).

On the other hand, the membrane area requirement is affected by changes in δ, P_{h}, K_1, or Q^{f}, even when γ_is, Pr, and the flow pattern are the same. However, the dimensionless area $\bar{A}$ is affected only by changes in γ_is, Pr, or the flow pattern.

RESULTS AND DISCUSSION

The separation of air (binary mixture) in a single-stage permeation unit, first discussed by Walawender and Stern (7), was numerically simulated for all four flow geometries by methods discussed in the present study. For ease of comparison, the operating conditions and the permeabilities were the same as taken by them (Table 1). The results are shown in Figs. 2 and 3, and they are in excellent agreement with the previous results.

Separation of the multicomponent gas mixture (Table 2), simulated by Shindo et al. (3) in their study for the full mixing case, was simulated by the alternative method presented here. The results were identical, as can be seen from Fig. 4.

Numerical simulation for the separation of a multicomponent gas mixture (Table 3) through a PVTM membrane was carried out for various flow geometries and operating conditions (expressed in terms of dimensionless variables). The effects of varying 1) the stage cut for a constant pressure

TABLE 1
Operating Parameters for Separation of Air, Taken from Walawender and Stern (7)

P_h	380 cmHg
P_l	76 cmHg
K_1 (oxygen)	$5 \times 10^{-8} \dfrac{\text{cm}^3\text{(STP)}\cdot\text{cm}}{\text{s}\cdot\text{cm}^2\cdot\text{cmHg}}$
K_2 (nitrogen)	$5 \times 10^{-9} \dfrac{\text{cm}^3\text{(STP)}\cdot\text{cm}}{\text{s}\cdot\text{cm}^2\cdot\text{cmHg}}$
Q^f	1×10^6 cm³/s
x_1^f	0.209
x_2^f	0.791
δ	2.54×10^{-3} cm

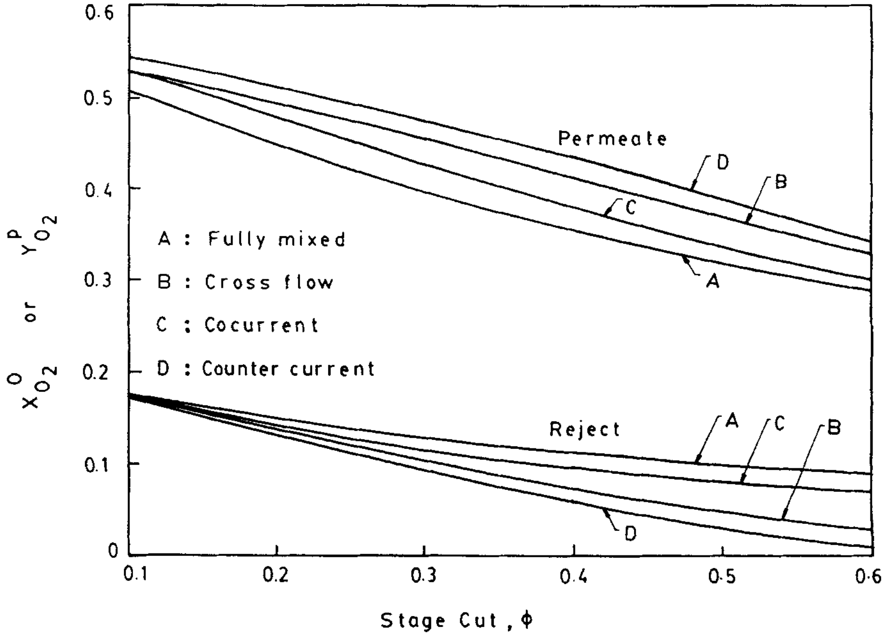

FIG. 2 Variation of outlet mole fraction with respect to the stage cut for a binary mixture of oxygen and nitrogen.

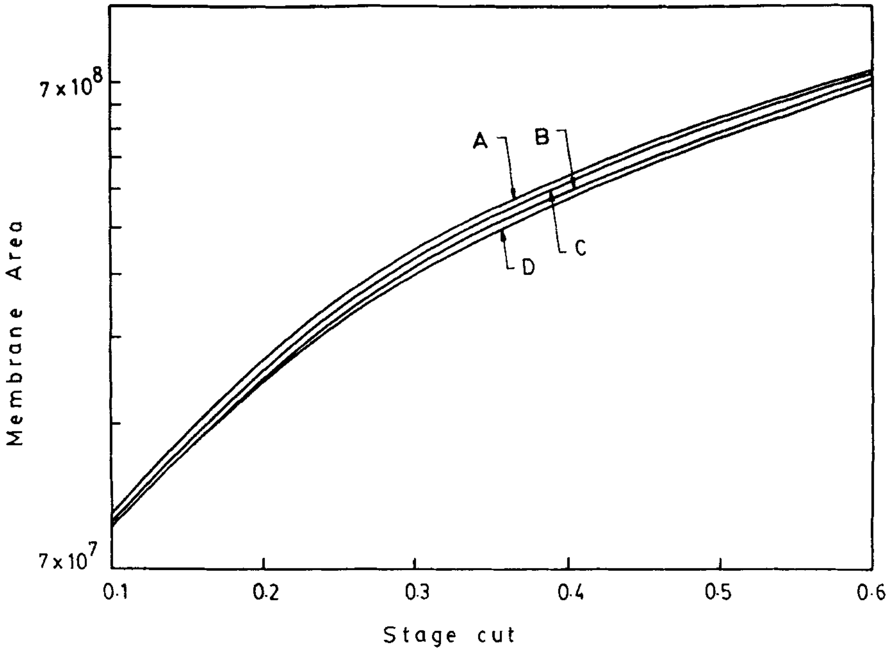

FIG. 3 Variation of membrane area required with respect to the stage cut for a binary mixture of oxygen and nitrogen.

ratio (Figs. 5 and 6), 2) the pressure ratio for a constant value of stage cut (Figs. 7 and 8), and 3) the pressure ratio for a constant area (Figs. 9 and 10) were studied.

For a constant value of Pr (50/380 = 0.132), the stage cut was varied and its effect on the area requirement as well as on the outlet concentrations on

TABLE 2
Operating Parameters for Separation of a Multicomponent Mixture, Taken from Shindo et al. (3)

Sample	Gas	Permeability $\left[\frac{\text{gmol}}{\text{s·m·Pa}}\right]$	Mole fraction at the inlet
1	Hydrogen	71.4	0.02
2	Methane	27.1	0.40
3	Carbon monoxide	20.6	0.10
4	Carbon dioxide	18.5	0.48

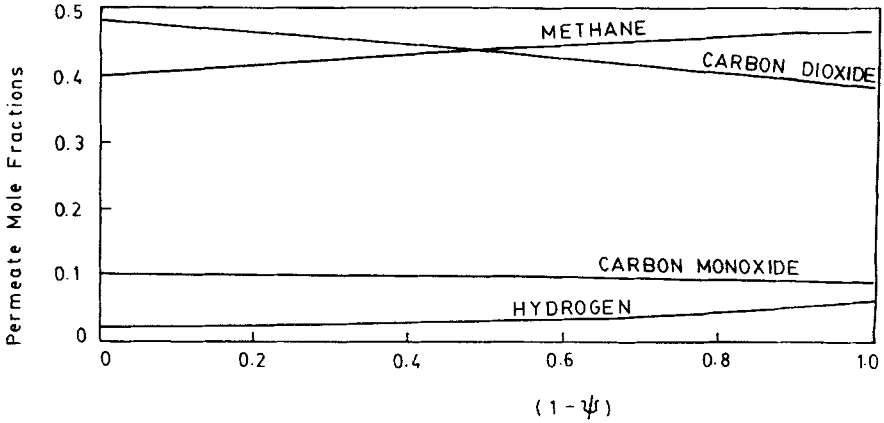

FIG. 4 Variation of outlet mole fractions on permeate side with respect to (1 − ψ) for the multicomponent gas mixture containing hydrogen, methane, carbon monoxide and carbon dioxide for full mixing flow geometry.

the permeate and the retentate side were observed. For low values of stage cut, all the flow geometries indicated similar results. The area requirement for full mixing flow geometry was the largest. The order of the area requirements was found to be

Full mixing flow > Cocurrent flow > Crossflow > Countercurrent flow

The area requirements (Fig. 6) for cocurrent flow countercurrent flow, and crossflow geometries, i.e., the plug flow geometries, were closer to each other than to the full mixing flow geometry. At higher stage cuts the full mixing flow case was distinctly inferior in terms of both lower separations and higher area requirements.

TABLE 3
Operating Parameters for Separation of a Multicomponent Mixture, Permeabilities Taken from Plate et al. (10)

Sample	Gas	Permeability × $10^7 \left[\frac{\text{cm}^3\cdot\text{cm}}{\text{cm}^2\cdot\text{s}\cdot\text{cmHg}}\right]$	Mole fraction at the inlet
1	Hydrogen	0.2	0.10
2	Nitrogen	0.11	0.23
3	Oxygen	0.044	0.40
4	Methane	0.013	0.27

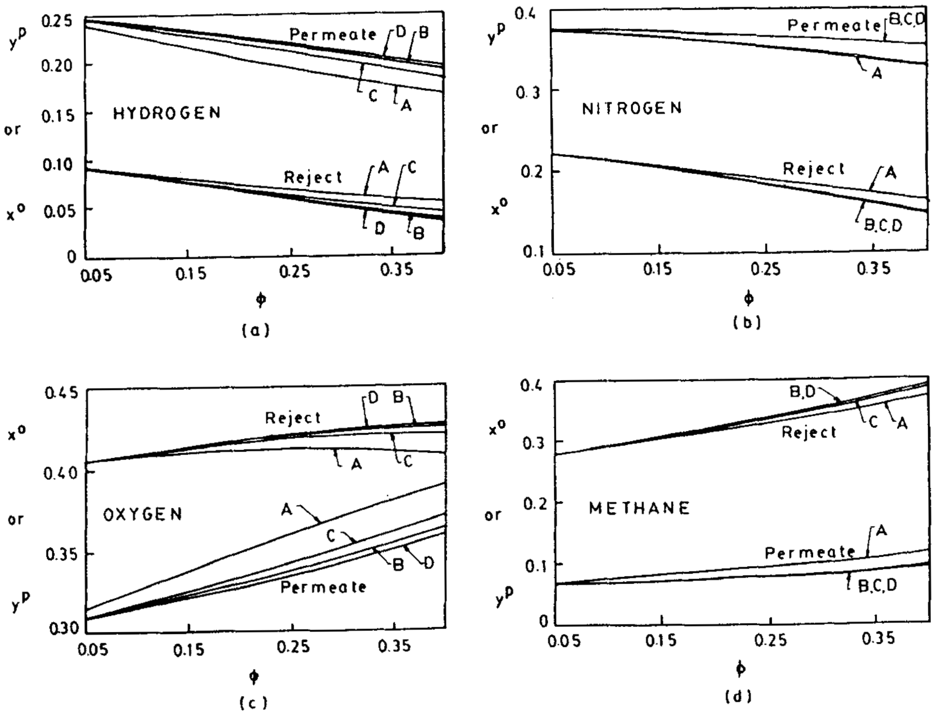

FIG. 5 Variation of the outlet mole fractions of a multicomponent gas mixture containing hydrogen, nitrogen, oxygen, and methane with respect to the stage cut for a constant pressure ratio (Pr = 50/380) and for various flow geometries: A = fully mixed, B = crossflow, C = cocurrent, D = countercurrent.

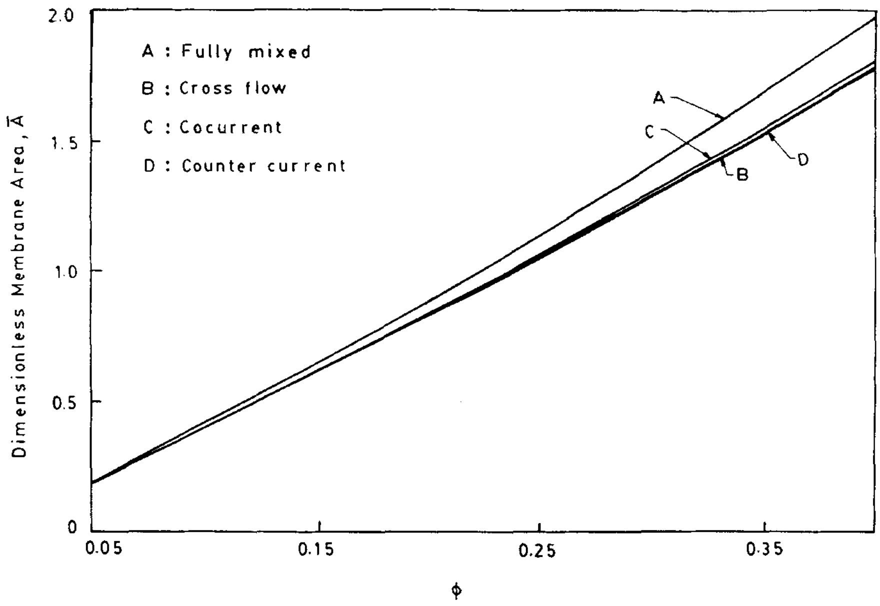

FIG. 6 Variation of dimensionless membrane area with respect to the stage cut for a constant pressure ratio (Pr = 50/380) and for various flow geometries.

The most permeable component (hydrogen) was always enriched. There was a distinct difference (Fig. 5a) in the outlet hydrogen mole fractions for different flow geometries. The permeate side outlet mole fractions varied in the order

Countercurrent flow > Crossflow > Cocurrent flow > Full mixing flow

The mole fractions for nitrogen, the second most permeable component, also behaved in a similar manner (Fig. 5b) except for the fact that its enrichment was less. However, this result cannot be generalized to all systems. Argon (Fig. 5c) showed no general trends and was enriched or depleted depending upon the operating conditions. Methane, the least permeable component, was always depleted (Fig. 5d). The mole fractions on the permeate side outlet varied in the order

Full mixing flow > Cocurrent flow > Crossflow > Countercurrent flow

The following observations were made on keeping the stage cut constant at $\phi = 0.4$ and varying the Pr.

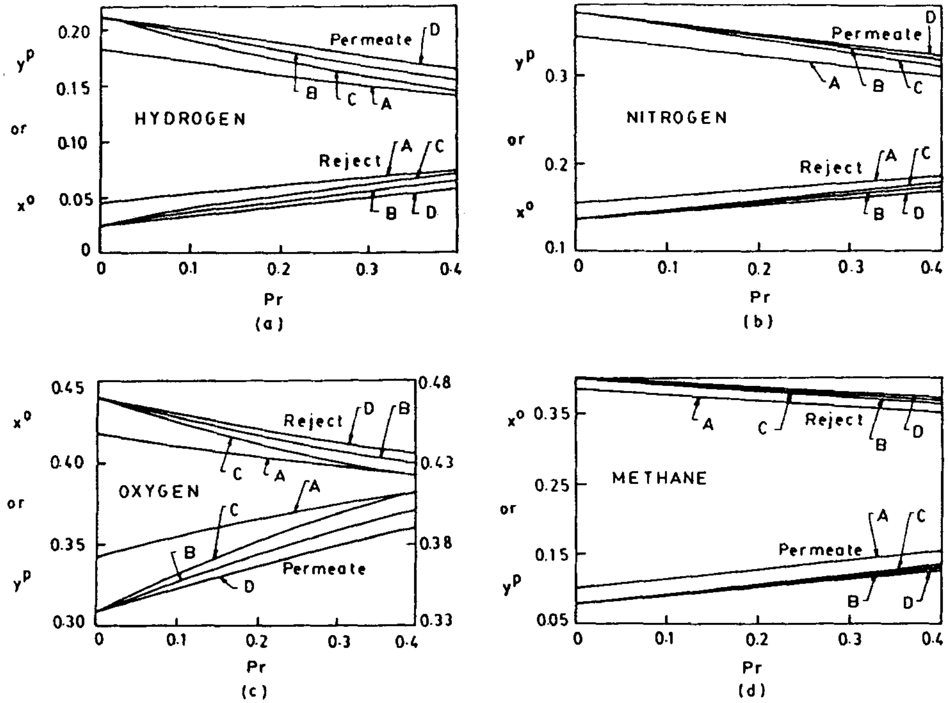

FIG. 7 Variation of the outlet mole fractions of a multicomponent gas mixture containing hydrogen, nitrogen, oxygen, and methane with respect to the pressure ratio for a constant stage cut ($\phi = 0.4$) and for various flow geometries: A = fully mixed, B = crossflow, C = cocurrent, D = countercurrent.

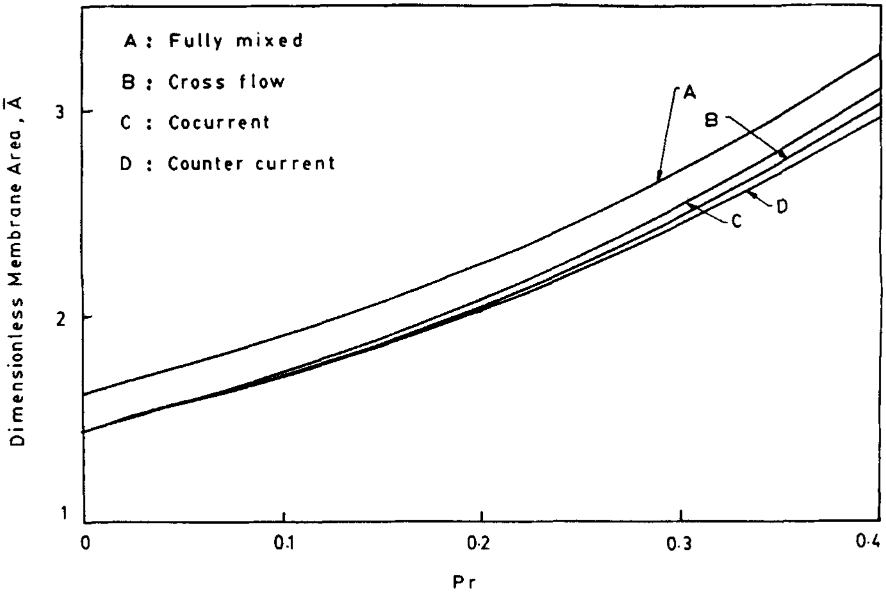

FIG. 8 Variation of dimensionless membrane area with respect to the pressure ratio for a constant stage cut (ϕ = 0.4) and for various flow geometries.

As seen in Figs. 7 and 8 for the limiting case when Pr → 0, all three plug flow geometries gave identical results for both outlet compositions and area requirements. However, this was not true for higher values of Pr. At any value of Pr the area requirements (Fig. 8) were again in the order

Full mixing flow > Cocurrent flow > Crossflow > Countercurrent flow

At low values of Pr the full mixing flow case gave distinctly different results, but at higher values became similar to crossflow. It is not clear if this result can be generalized. The variation of mole fractions of individual gases for constant ϕ (Fig. 7) were similar to the case of constant Pr.

The effect of variation of Pr when the area is constant ($\bar{A}$ = 1.824) showed (Fig. 10) that the stage cut for different flow geometries were in the order

Countercurrent flow > Crossflow > Cocurrent flow > Full mixing flow

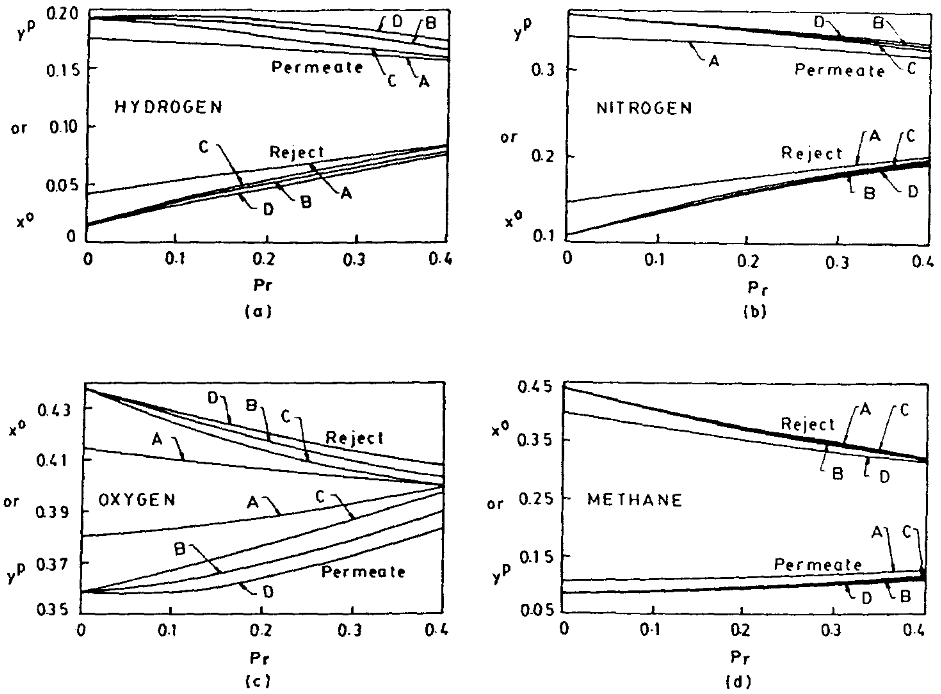

FIG. 9 Variation of the outlet mole fractions of a multicomponent gas mixture containing hydrogen, nitrogen, oxygen, and methane with respect to the pressure ratio for a constant dimensionless area (A = 1.824) and for various flow geometries: A = fully mixed, B = crossflow, C = cocurrent, D = countercurrent.

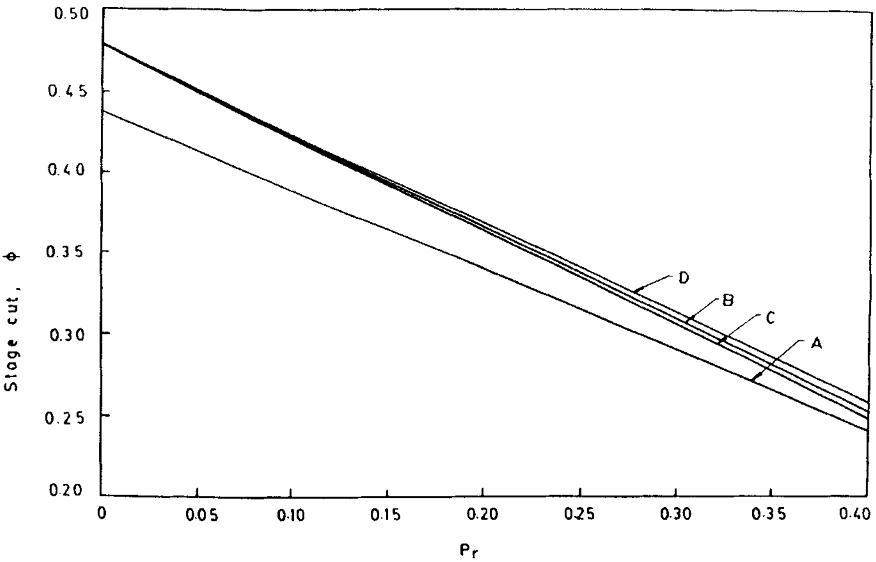

FIG. 10 Variation of dimensionless membrane area with respect to the pressure ratio for a constant dimensionless area ($\bar{A}$ = 1.824) and for various flow geometries: A = fully mixed, B = crossflow, C = cocurrent, D = countercurrent.

The variations in mole fractions on varying Pr showed (Fig. 9) the same trends as observed in the case when the stage cut was constant.

CONCLUSIONS

Given the inlet feed conditions, the operating conditions, the flow geometry, the outlet mole fractions, and the flow rates can be predicted by the use of the numerical simulation techniques discussed in the present study. The value of either the membrane area or the stage cut must be known, and given one, the other can be calculated.

The important conclusions which can be derived from the present study are:

1. The complete set of operating conditions can be represented through the dimensionless variables Pr and γ_is along with either ϕ or $\bar{A}$ (whichever is known) and the flow geometry.
2. For all the flow geometries the most permeable component is always enriched in the permeate stream and the least permeable component is always depleted. The intermediate components (i = 2, 3, . . . ,

$n - 1$) may be enriched or depleted depending upon the operating conditions.

3. The efficiency of separation varies in the order

Countercurrent flow ≥ Crossflow ≥ Cocurrent flow ≥ Full mixing flow

However, when Pr → 0, the plug flow geometries tend to become identical. In other words, at very low values of Pr their outlet compositions and flow rates converge to the same value.

4. At higher values of Pr the efficiency of separation is reduced and the outlet compositions for various flow geometries become nearly the same.

APPENDIX 1

Limiting Values of Stage Cut and Area in Full Mixing Case

In multicomponent gas separation the most permeable component is always enriched (3), i.e.,

$$y_1^p > x_1^o \tag{A1-1}$$

while the least permeable component ($i = n$) is always depleted,

$$y_n^p < x_n^o \tag{A1-2}$$

Hence, for the most permeable component in the full mixing case:

$$Q^f \phi y_1^p = \frac{K_1 A}{\delta}(P_h x_1^o - P_l y_1^p) \tag{A1-3}$$

and from Eqs. (A1-1) and (A1-3):

$$\frac{K_1 A}{\delta \phi Q^f} > \frac{1}{P_h - P_l} \tag{A1-4}$$

For the least permeable component,

$$Q^f \phi y_n^p = \frac{K_n A}{\delta}(P_h x_n^o - P_l y_n^p) \tag{A1-5}$$

and from Eqs. (A1-2) and (A1-5) we get

$$\frac{K_n A}{\delta \phi Q^f} < \frac{1}{P_h - P_l} \tag{A1-6}$$

For the case of known stage cut from Eqs. (A1-3) and (A1-6), we obtain the limits on A as

$$\frac{\delta\phi Q^{\mathrm{f}}}{K_1(P_{\mathrm{h}} - P_{\mathrm{l}})} < A < \frac{\delta\phi Q^{\mathrm{f}}}{K_1(P_{\mathrm{h}} - P_{\mathrm{l}})}\frac{K_1}{K_n} \tag{A1-7}$$

or in the dimensionless form

$$\frac{\phi}{1 - \mathrm{Pr}} < \bar{A} < \frac{\phi}{1 - \mathrm{Pr}}\frac{K_1}{K_n} \tag{A1-8}$$

Similarly, for the case of known area we have

$$\frac{K_n}{K_1}\frac{K_1(P_{\mathrm{h}} - P_{\mathrm{l}})A}{\delta Q^{\mathrm{f}}} < \phi < \frac{K_1(P_{\mathrm{h}} - P_{\mathrm{l}})A}{\delta Q^{\mathrm{f}}} \tag{A1-9}$$

which in dimensionless form can be written as

$$\frac{K_n}{K_1}\bar{A}(1 - \mathrm{Pr}) < \phi < \bar{A}(1 - \mathrm{Pr}) \tag{A1-10}$$

Moreover, for the steady state

$$0 < \phi < 1 \tag{A1-11}$$

Equations (A1-9) and (A1-10) along with Eq. (A1-11) constitute the limits within which ϕ can vary.

APPENDIX 2

Method of Calculation for a Differential Volume Element with No Inflow Parallel to Membrane on Permeate Side

When there is no gas flow into the differential volume element on the permeate side parallel to the membrane, y_is can be evaluated for the given set of x_is by the following method.

Applying Eq. (14) for ith and jth component:

$$y_i\frac{dq^{\mathrm{l}}}{dA} = \frac{K_i}{\delta}(P_{\mathrm{h}}x_i - P_{\mathrm{l}}y_i) \tag{A2-1}$$

$$y_j\frac{dq^{\mathrm{l}}}{dA} = \frac{K_j}{\delta}(P_{\mathrm{h}}x_j - P_{\mathrm{l}}y_j) \tag{A2-2}$$

Also from Eq. (15):

$$\frac{dq^{\mathrm{l}}}{dA} = \sum_{i=1}^{n}\left[\frac{K_i}{\delta}(P_{\mathrm{h}}x_i - P_{\mathrm{l}}y_i)\right] \tag{A2-3}$$

Dividing Eq. (A2-2) by Eq. (A2-1) and using Eq. (39):

$$\frac{y_j}{y_i} = \frac{K_j(x_j - \mathrm{Pr}y_j)}{K_i(x_i - \mathrm{Pr}y_i)} \tag{A2-4}$$

$$y_j = \frac{y_i x_j K_j}{K_j \mathrm{Pr} y_i + K_i(x_i - \mathrm{Pr} y_i)} \tag{A2-5}$$

Using Eqs. (A2-1) and (A2-3):

$$y_i = \frac{K_i(x_i - \mathrm{Pr} y_i)}{\sum_{j=1}^{n} K_j(x_j - \mathrm{Pr} y_j)} \tag{A2-6}$$

From Eqs. (A2-5) and (A2-6):

$$y_i = \frac{K_i(x_i - \mathrm{Pr} y_i)}{\sum_{j=1}^{n} K_j \left(x_j - \dfrac{\mathrm{Pr} y_i x_j K_j}{K_j \mathrm{Pr} y_i + K_i(x_i - \mathrm{Pr} y_i)} \right)} \tag{A2-7}$$

Now, using Eq. (40), Eq. (A2-7) becomes

$$y_i = \frac{\gamma_i(x_i - \mathrm{Pr} y_i)}{\sum_{j=i}^{n} \gamma_j \left(x_j - \dfrac{\mathrm{Pr} y_i x_j \gamma_j}{\gamma_j \mathrm{Pr} y_i + \gamma_i(x_i - \mathrm{Pr} y_i)} \right)} \tag{A2-8}$$

Equation (A2-7) can symbolically be represented as

$$y_i = g(\{x_i\}, \{K_i\}, \mathrm{Pr}, y_i) \tag{A2-9}$$

Since $\{x_i\}$, $\{K_i\}$, and Pr are known, Eq. (A2-9) contains only one unknown, y_i.

Consider the most permeable component ($i = 1$). It is known that $y_1 > x_1$ and $y_1 < 1$, so Eq. (A2-8) can be numerically solved between these limits to the desired level of accuracy by the method identical to that used for solving Eq. (11) to obtain the value of y_1.

By using Eq. (A2-5), $\{y_j\}$ can be computed. In other words, y_j can be obtained if the numerical values of process variables and retentate side mole fractions are known, i.e.,

$$y_i = f(\{x_i\}, \mathrm{Pr}) \tag{A2-10}$$

NOMENCLATURE

n	number of components
A	area
K_i	permeability of the ith component
P_{h}	total pressure on the high pressure side
P_{l}	total pressure on the permeate side

Pr	pressure ratio P_l/P_h
Q^f	feed flow rate
Q^o	reject flow rate
Q^p	permeate flow rate
W	width of the membrane
$\overline{A}$	dimensionless area
q^h	flow rate at any point on the high pressure side
q^l	flow rate at any point on the low pressure side
$\overline{q}^h$	dimensionless flow rate at any point on the high pressure side
x_i^f	mole fraction of the ith component in feed
x_i^o	mole fraction of the ith component in reject.
y_i^p	mole fraction of the ith component in permeate
x_i	variable mole fraction of ith component on the high pressure side at any point
y_i	variable mole fraction of the ith component on low pressure side at any point

Greek

ϕ	stage cut
δ	thickness
γ_i	permeability ratio with respect to the most permeable component
$\{\ \}$	the set of values for all components, e.g., $\{x_i\}$, $\{y_i\}$, etc.

Subscripts

i, j, k	i, j, and kth component
h	high
l	low

Superscripts

f	feed
o	outlet on reject side
p	permeate

REFERENCES

1. C. T. Blaisdell and K. Kammermeyer, "Countercurrent and Cocurrent Gas Separation," *Chem. Eng. Sci.*, *28*(6), 1249–1255 (1973).
2. R. W. Naylor and P. O. Becker, "Enrichment Calculations in Gaseous Diffusion: Large Separation Factor," *AIChE J.*, *1*(1), 95–99 (1955).

3. Y. Shindo, N. Itoh, and K. Harya, "A Theoretical Analysis of Multicomponent Gas Separation by Means of a Membrane with Perfect Mixing," *Sep. Sci. Technol.*, *24*(7&8), 599–616 (1989).
4. S. A. Stern, "Gas Permeation Process," in *Industrial Processing with Membranes* (R. E. Larey and S. Loeb, Eds.), Wiley-Interscience, New York, 1971.
5. S. A. Stern, "Separation of Gases by Selective Permeation," in *Membrane Separation Process* (P. Meares, Ed.), Elsevier Scientific, 1976.
6. L. Tranchino, R. Santarossa, F. Carta, C. Fabiani, and L. Bimbi, "Gas Separation in a Membrane Unit: Experimental Results and Theoretical Predictions," *Sep. Sci. Technol.*, *24*(14), 1207–1229 (1989).
7. W. P. Walawender and S. A. Stern, "Analysis of Membrane Separation Parameters. II: Countercurrent and Cocurrent Flow in a Single Permeation Stage," *Sep. Sci.*, *7*(5), 553–584 (1972).
8. S. Weller and W. A. Steiner, "Separation of Gases by Fractional Permeation through Membranes," *J. Appl. Phys.*, *21*, 279–282 (1950).
9. C. Y. Pan and H. W. Habgood, "An Analysis of the Single Stage Gaseous Permeation Process," *Ind. Eng. Chem., Fundam.*, *13*(4), 323–331 (1974).
10. N. A. Plate, A. K. Bokarev, N. E. Kaliuzhnyi, E. G. Litvinova, V. S. Khotimskii, V. V. Volkov, and Yu. P. Yampolskii, "Gas and Vapor Permeation and Sorption in Poly(Trimethylsilylpropyne)," *J. Membr. Sci.*, *60*, 13–24 (1991).
11. M. K. Jain, S. R. K. Iyengar, and R. K. Jain, *Numerical Methods for Scientific and Engineering Computation*, 2nd ed., Wiley Eastern, 1987.

Received by editor October 3, 1994